

## DESIGN AND CALIBRATION OF FALSE BAY SEDIMENT MODEL

by

J S Schoonees\* and J P Möller\*\*

### 1. INTRODUCTION

False Bay is situated near Cape Town in the Republic of South Africa. The National Research Institute for Oceanology (NRIO) of the Council for Scientific and Industrial Research (CSIR) was commissioned to undertake studies on a recreational scheme in the Strandfontein area of False Bay. A tidal pool was built as phase 1 of this project. Phase 2 is a bathing improvement scheme (see Figures 1 and 2).

The aim of the bathing improvement scheme which consists of a number of structures, is to provide bathing facilities for the Mitchell's Plain community. At present the major part of the coast is rather unsafe for bathing mainly because of very steep beach profiles. Conditions were laid down to ensure safe bathing, e.g. a uniform flat beach slope and the absence of rock and rip currents. Further requirements were that a safe bathing beach must be formed soon after completion of the structures and that the adjacent coastline must not be adversely affected in the long term. This paper deals with the design and calibration of a sediment model which was chosen to evaluate and optimise the design of the proposed T-groyne and the system of detached breakwaters shown in Figure 3.

### 2. DESIGN OF THE MODEL

#### 2.1 Design Philosophy

The basic prerequisite of a sediment model is to reproduce sediment motion correctly. This can be achieved by

---

\* J S Schoonees, Sediment Dynamics Division, Coastal Engineering and Hydraulics, National Research Institute for Oceanology, South African Council for Scientific and Industrial Research, Stellenbosch.

\*\* J P Möller, Sediment Dynamics Division, Coastal Engineering and Hydraulics, National Research Institute for Oceanology, South African Council for Scientific and Industrial Research, Stellenbosch.

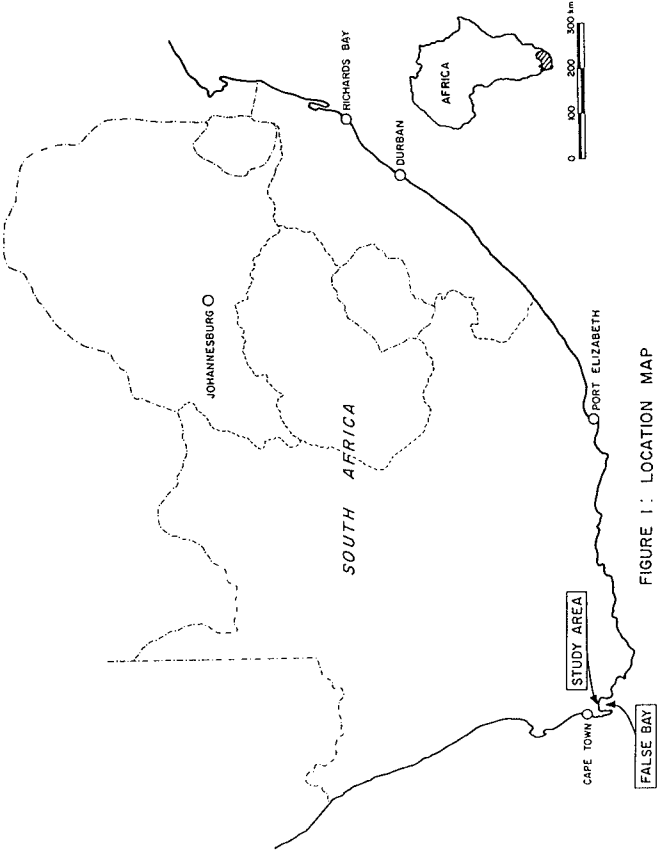
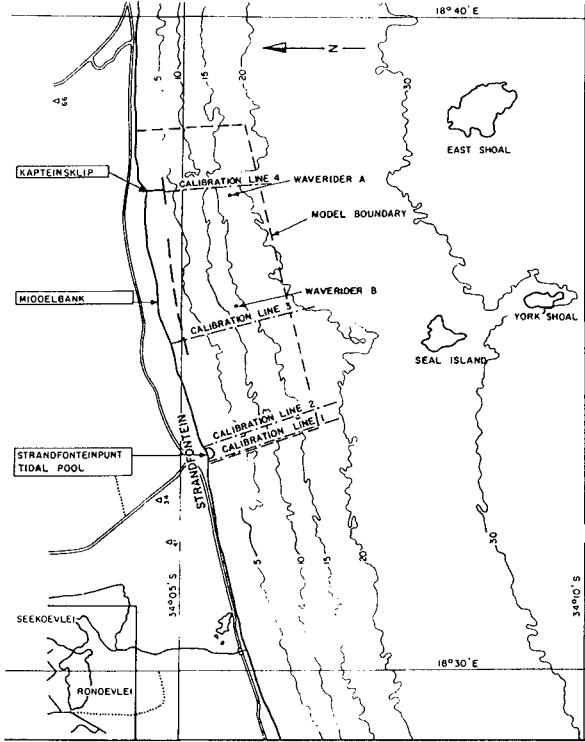


FIGURE 1: LOCATION MAP



FIGURE 2: STUDY AREA



LEGEND:  
 \* SCALE 1:75 000  
 \* DEPTHS IN m TO CHART DATUM (MSL - 0,90m)  
 \* ONLY APPROXIMATE CONTOURS GIVEN

FIGURE 3: THE BATHING IMPROVEMENT SCHEME

modelling the on-offshore and longshore transport rates accurately. Inherent in this approach is the fact that the sedimentological time scale must not vary from place to place in the model. The time scale must also be constant in time, that is, as the experiment progresses. It will be shown that the selection of the bed material and the determination of the horizontal and vertical scales after model boundaries have been chosen, will ensure that sediment motion is correctly modelled and that a constant sedimentological time scale is obtained.

## 2.2 Choice of the Bed Material

Sand instead of lightweight material was chosen as the most suitable sediment for the model for the following reasons:

(a) To obtain the most accurate simulation of longshore transport the functional relationship between the transport and the driving forces should be examined. This relationship can, for most practical purposes, be approximated as:

$$S_x = a(v_* - v_{*c})^b \quad (1)$$

where a, b = coefficients dependent on the grain size

$v_*$  = shear velocity

$v_{*c}$  = critical shear velocity at initiation  
of particle motion

$S_x$  = longshore transport rate.

The best comparison between transport rates in model and prototype is obtained when  $v_{*c}$  and b are scaled 1 to 1. This can be done only by using sand for model material with approximately the same grain size as in prototype because  $v_{*c}$  and b are dependent on the grain size. The scale of  $v_*$  depends on the velocity scale and the hydraulic roughness scale. Bedforms are exaggerated in the model relative to prototype; this results in a roughness scale which is closer to unity than to the vertical scale. Consequently, more material is entrained on scale, due to higher turbulence close to the bed, than in prototype. The scaling process for longshore transport is completed by choosing a scale for the longshore current velocity which yields a velocity greater than that which would have been obtained from the Froude velocity scale in order to ensure a constant time scale. This is similar to the concept of an "ideal velocity scale" introduced earlier by Bijker (1967).

(b) It has been shown (Swart, 1974) that the geometric shape of the dynamic beach profile depends strongly on the grain size, wave height and wave steepness. Lightweight material, scaled according to the submerged weight, will be relatively too heavy out of the water, resulting in very steep (almost vertical) beach slopes near the water line. Therefore, to ensure the same breaker type in the model and

prototype and consequently also similar longshore current profiles, sand with the same grain size as the prototype material should be used.

The empirically derived relationship (Swart, 1974) for the equilibrium beach slope of sandy beaches is as follows:

$$m_r = 1,51 \times 10^3 \left(\frac{H_0}{L_0}\right)^{-1} [H_0^{0,132} D_{50}^{-0,447} \left(\frac{H_0}{L_0}\right)^{-0,717}]^{-2,38} + 0,11 \times 10^{-3} \left(\frac{H_0}{L_0}\right)^{-1} \quad (2)$$

where  $m_r$  = schematized equilibrium beach slope at the still water level

$H_0$  = deep-water wave height

$L_0$  = deep-water wave length

$D_{50}$  = median sediment particle diameter.

(c) Porosity is normally greater at the grain sizes needed to model sedimentary processes with lightweight material than in prototype. Therefore substantial wave energy losses occur due to percolation. The correct modelling of the breaker characteristics and longshore water and sediment movement becomes extremely difficult to achieve in practice.

### 2.3 Selection of the Model Boundaries

The study area stretching from a slightly curved beach to the 22 m contour, is naturally bounded by two easily distinguishable features, namely, the tidal pool at Strandfonteinpunt and the rocks of Kapteinsklip - see Figure 3. Both of these form a partial obstruction to the longshore transport. The natural choice for the model boundaries is therefore as follows:

(a) From Strandfonteinpunt to approximately 1 km beyond Kapteinsklip. It was necessary to extend the model to the east of Kapteinsklip because the proposed scheme incorporates a groyne at Kapteinsklip.

(b) The depth at the offshore limit of the model is 22 m relative to mean sea level (MSL) but the movable bed terminates at the 16 m contour. This is safely beyond 8 m, the depth of significant sediment movement found in a theoretical analysis of longshore transport in a feasibility study.

### 2.4 Determination of the Horizontal and Vertical Scales of The Model

Swart (1974) devised a method to calculate the on-offshore transport that is based on the equilibrium beach profile concept. According to Swart (1974) the on-offshore trans-

port is directly proportional to the difference in configuration between the existing and equilibrium profiles. Therefore to model on-offshore transport correctly, the distortion of the model (ratio between the vertical and horizontal scales) must be equal to the ratio between the equilibrium beach slope in the model and that in prototype. This method was proposed by Bijker (1967) as well as Fan and Le Méhauté (1969). The Swart (1974) procedure for the calculation of the equilibrium beach slope was used. If the above-mentioned criterion is not met, additional on-offshore transport will take place in the model because of the incorrect distortion of the model - something that does not happen in prototype.

A horizontal scale of 1 in 120 was chosen to fit the model of the study area into the available model basin. From the results of the feasibility study the representative wave condition is: wave period = 10 s; deep-water significant wave height ( $H_S$ ) = 2 m. The vertical scale was computed to satisfy the previously mentioned criterion as follows:

(a) Determine the prototype equilibrium beach slope:

From (2)  $m_{r,p^\infty} = 0,0240$  with  $D_{50,p} = 450 \mu\text{m}$  and  $L_O = \frac{gT^2}{2\pi} = 156 \text{ m}$  (linear theory).

(g = gravitational acceleration; T = wave period; subscripts: m = model; p = prototype;  $\infty$  = infinitely long time, that is, equilibrium conditions.)

(b) Select a vertical scale, say, 1 in 40.

(c) Calculate the equilibrium beach slope in the model with:

$$H_{S,m} = \frac{1}{40} \times 2 = 0,05 \text{ m}$$

$L_{O,m} = \frac{1}{40} \times 156 = 3,90 \text{ m}$  (the wave length must be scaled with the vertical scale in order to model refraction correctly).

$D_{50,m} = 450 \mu\text{m}$  ( $D_{50}$  must preferably be as close as possible to  $D_{50,p}$ , except for very coarse prototype material. For  $D_{50,p}$  large,  $D_{50,m}$  must be chosen such that  $D_{50,m} < D_{50,p}$  or problems with the initiation of sediment movement will occur.

From (2):  $m_{r,m^\infty} = 0,0491$

(d) Check whether the slope ratio ( $\frac{m_{r,m^\infty}}{m_{r,p^\infty}}$ ) is equal to the distortion factor (DF).

$$DF = \frac{1}{40} / \frac{1}{120} = 3,0$$

$$\frac{m_{r,m^\infty}}{m_{r,p^\infty}} = \frac{0,0491}{0,0240} = 2,04 \neq DF.$$

Choose a new vertical scale and repeat the procedure until

$\frac{m_{r,m^\infty}}{m_{r,p^\infty}} = DF$ . The result of this iteration process was a vertical scale of approximately 1 in 50. It must be added, because (2) is applicable only to sandy beaches, that the sediment in the model must be sand to permit the use of this method.

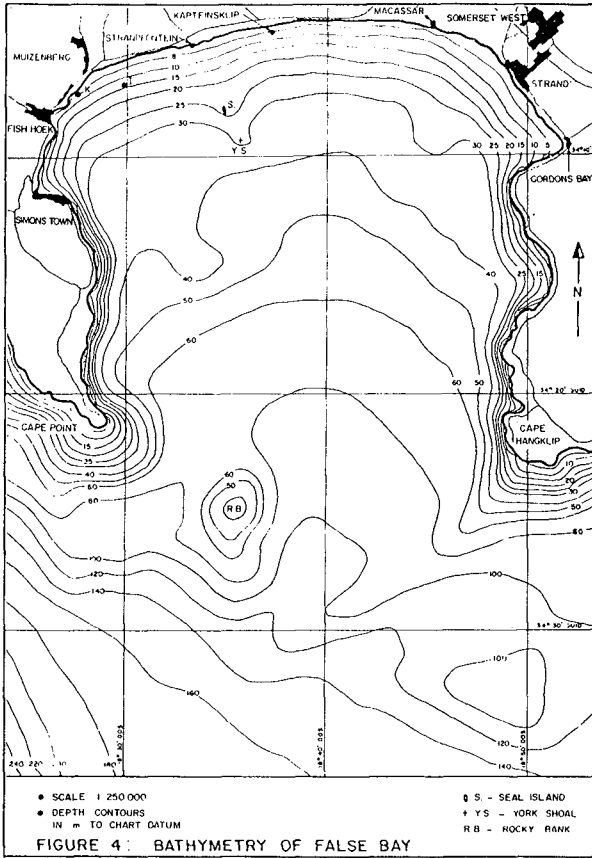
(f) Check that a realistic vertical scale is obtained by quantifying the internal friction and surface tension effects. If not, change the horizontal scale and repeat the iteration process.

Because it is a distorted model with the beach slope being steeper than in prototype, the breaker index will be influenced in such a manner that the breaker line will move inshore. To compensate for this effect, the wave height was increased to scale the width of the breaker zone correctly. This increase was, however, not significant enough to conflict with the requirements described in previous paragraphs.

### 3. DATA ACQUISITION AND CALIBRATION

#### 3.1 Waves

Datawell Waveriders (accelerometer buoys) were deployed at the site to measure the wave heights and periods. Partly because of the complex bathymetry (see Figures 3 and 4) of the bay which caused unreliability of the theoretical refraction method used, and partly to obtain the best possible coverage in the limited recording period available (one year only - April 1980 to March 1981), recordings were made at two separate locations in a water depth to mean sea level (MSL) of approximately 20 m (see Figure 3 for the positions of the Waveriders). The results are summarized in Figures 5 and 6. Simultaneously a year-long exercise was undertaken during which aerial photographs were obtained of the study area approximately every second day. By orientating the individual photographs taken during each flight with the aid of a template, photographic strips of the coastline were obtained. The wave directions along the 6 m depth contour were then read off from these strips, thus acquiring a wave direction distribution along the coastline for every flight. The accuracy of this method, obtained from successive flights on two occasions (total number of repetitions: 48 flights) is 3,8°.



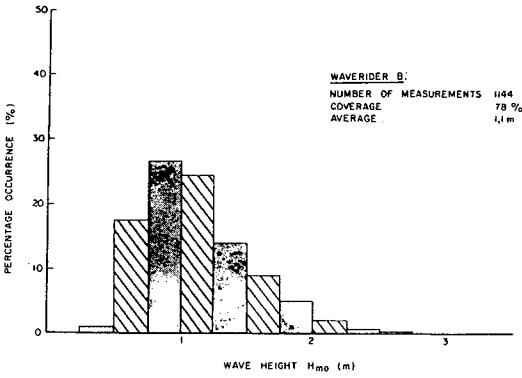
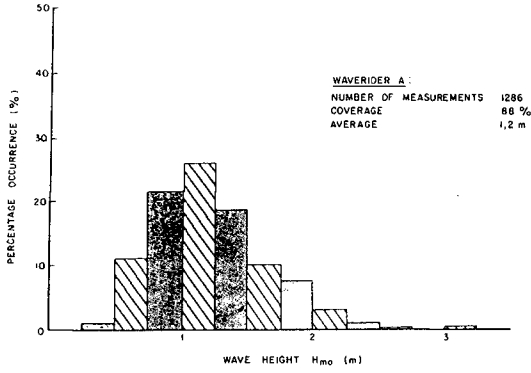


FIGURE 5: WAVE HEIGHT HISTOGRAMS

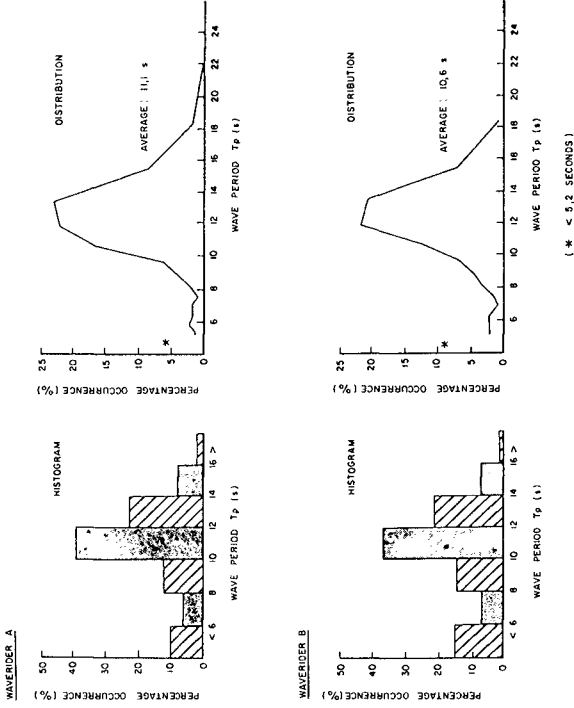


FIGURE 6 : WAVE PERIOD OCCURRENCE

Deep-sea wave directions during the (Waverider) recording year (see Figure 7) were obtained from voluntary observing ships. The wave direction distribution along the 6 m depth contour was then compared with the distribution obtained from the theoretical wave refraction exercise. The measured wave patterns proved the theoretically-predicted tendencies.

Deep-sea ship observations also provided the wave climate over a period of 20 years (1960-1979). Equivalent deep-sea instrument (Waverider) data were computed for the 20-year period by using the relations (CSIR, to be published in 1982):

$$H_s \text{ (Waverider)} = 1,0 + 0,55 H_s \text{ (ship)}$$

$$T_p \text{ (Waverider)} = 4,1 T^{0.55} \text{ (ship)}.$$

By shoaling and refracting each of these observations the shallow water wave climate at the position of waverider A (see Figure 3) was determined, thus making it possible to see how representative the year's recorded data were. The wave height exceedance curves are shown in Figure 8, which indicates a relatively calm recording year.

The wave climate was divided into two parts, that is, westerly waves (causing eastbound longshore transport) and easterly waves (causing westbound longshore transport). For example, the westerly waves include waves from the WSW, SW, etc. As the wave energy is proportional to the product of the peak energy wave period ( $T_p$ ) and the square of the significant wave height ( $H_s$ ), it was possible to calculate  $\overline{T_p}$  and  $\overline{H_s^2 T_p}$  for easterly and westerly waves (the bar denotes mean values). Thus a representative wave that has the average wave energy is one with  $H_s = (\overline{H_s^2 T_p} / \overline{T_p})^{1/2}$ . This was done for both easterly and westerly waves, resulting in:

$$H_{s,\text{east}} = 1,0 \text{ m}; T_{p,\text{east}} = 10,7 \text{ s}$$

$$H_{s,\text{west}} = 0,8 \text{ m}; T_{p,\text{west}} = 12,2 \text{ s}.$$

The wave directions along the model boundary were measured from refraction diagrams for all possible wave directions and wave periods and weighted mean directions along the boundary obtained by using the deep-sea wave climate. However, irregular waves are preferred to regular waves due to the fact that in prototype the breaker line is continually shifting, as opposed to the stationary breaker line resulting from regular waves. Furthermore, irregular waves in the model will also reduce secondary wave generation effects. By using a period variator the periods were randomly altered around the calculated peak wave period according to a normal distribution with a standard devia-

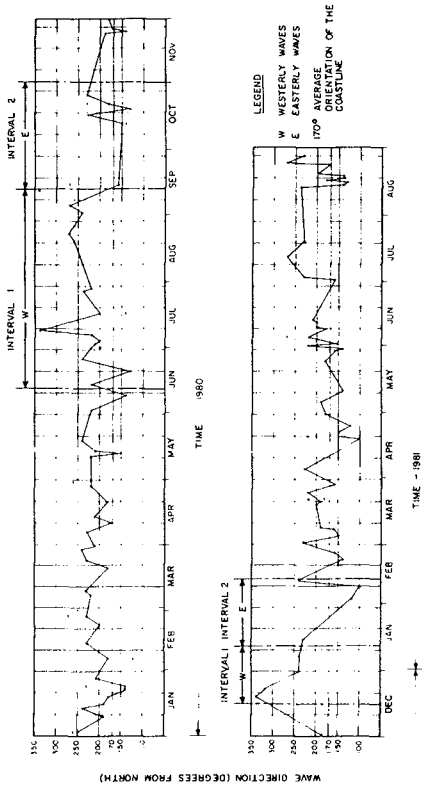


FIGURE 7 : DEEP SEA WAVE DIRECTIONS (SHIP DATA)



tion of 0,2 s. At the same time the wave height was changed in a cyclic manner, resulting in quasi-irregular waves. A series of measurements were taken to ensure the correct reproduction of the input wave variables.

Because the calculated wave characteristics and the model sediment size differ from the original values, the vertical scale was recalculated. The discrepancy between these two vertical scales was insignificant.

### 3.2 Tides

The tides in the False Bay area are semi-diurnal with a mean range of about 1,6 m. Because tidal currents are negligible in this area (Atkins, 1970) the other tidal effects, that is, exposure of a steeper part of the beach profile to wave action, as well as causing the breaker line to change position, were modelled by testing 0,5 m above MSL and using quasi-irregular waves.

### 3.3 Sediment

Sediment samples were taken monthly at fixed positions along the beach. The particle size and distribution were determined in a settling tube. The median particle diameter for the 8 km stretch of coastline (upper and lower foreshore combined) from February 1980 to November 1981 was 450  $\mu\text{m}$ . The beach between Strandfonteinpunt and Kapteinsklip is a moderately protected beach with little net sediment movement. Therefore it was difficult to acquire calibration data because quarterly hydrographic surveys showed beach and nearshore profile changes of less than 0,3 m (which approaches the measuring accuracy of the surveys). Figures 9 and 10 show typical beach and nearshore profiles. Daily aerial photographs used for determining the wave direction provided profile growth and recession rates at four places (see Figure 3 for the four calibration lines) along the coastline. After the scales of the photographs had been determined, the distances between the waterline and arbitrarily chosen beacons were measured. Tidal corrections, deduced from the beach profiles and the tidal heights at the time that the photographs were taken, were then applied to give the growth and recession of the waterline with time. Four distinct time intervals were identified from Figure 7, two for easterly and two for westerly waves. These, together with the corrected growth and recession rates are shown in Figures 11, 12 and 13. The rates of waterline movement were averaged for easterly and westerly waves at each of the calibration lines.

In order to model the prototype conditions, it was necessary to introduce and extract a longshore current as well as longshore sediment transport at the sides of the model.

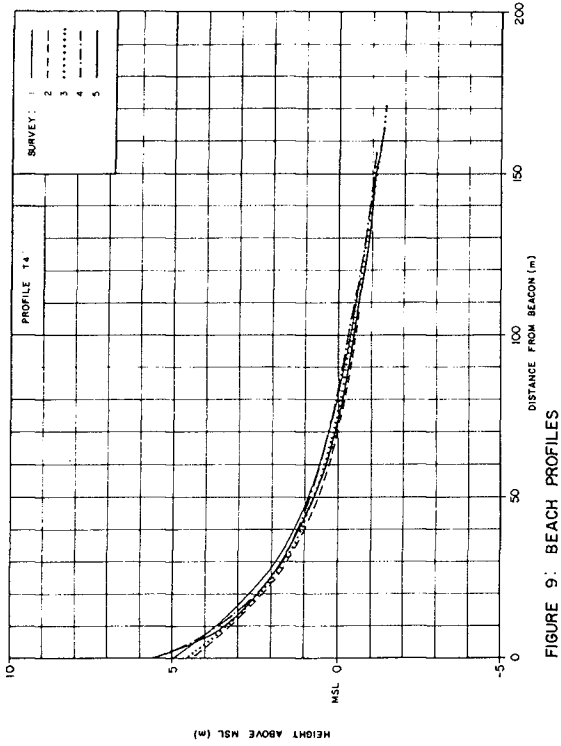


FIGURE 9: BEACH PROFILES

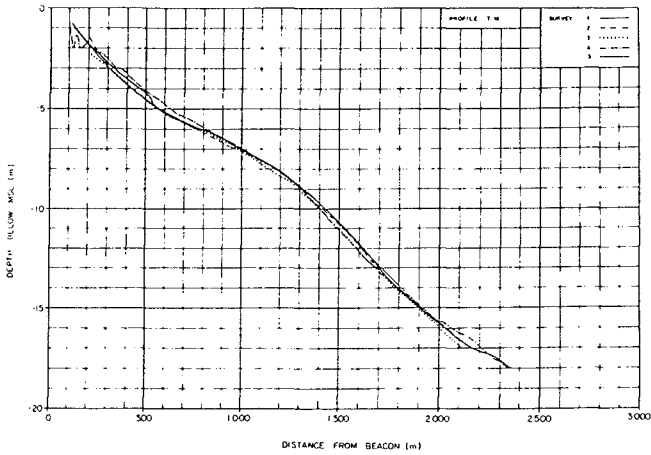


FIGURE 10: NEARSHORE PROFILES

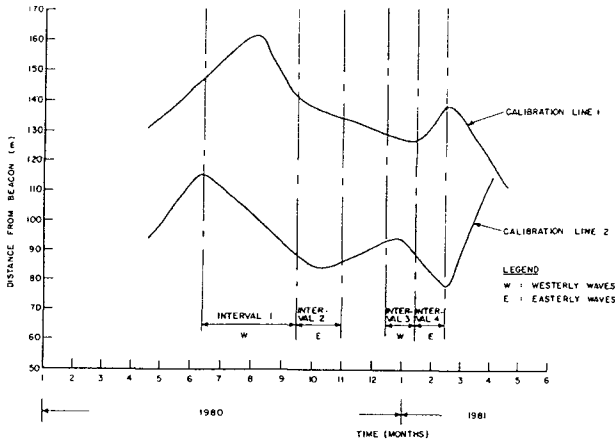


FIGURE 11: WATERLINE MOVEMENT AT STRANDFONTEINPUNT

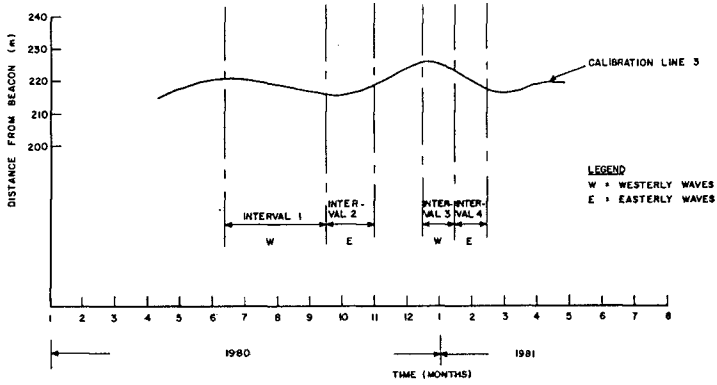


FIGURE 12: WATERLINE MOVEMENT AT MIDDELBANK

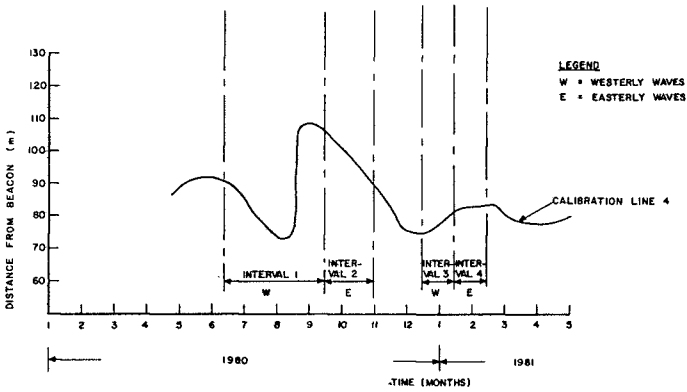


FIGURE 13: WATERLINE MOVEMENT AT KAPTEINSKLIP

Therefore the entrance/exit conditions had to be calibrated for both the easterly and westerly waves.

The overall water circulation pattern was monitored using a dye tracer to ensure the correct reproduction of the magnitude of the longshore current. The correct distribution of the longshore current (as predicted by Longuet-Higgins (1970)) relative to the average breaker line was obtained with a set of baffles. The sand feeding rate was determined by a trial and error process. It was found that because of the relatively slow longshore sediment movement, the feeding had to be intermittent. After these variables had been calibrated, verification tests were executed to determine the sedimentological time scale. The prototype tendencies of growth and recession were matched in the model except for calibration line 1. The proximity of this line to the edge of the model prevented its use during calibration procedure.

The distribution of the shallow-water wave climate according to wave direction, is as follows:

- (i) westerly waves: 46,9%,
- (ii) easterly waves: 13,2%,
- (iii) calm periods (includes deep water waves moving away from the land): 36,5%, and
- (iv) waves perpendicular to the coastline of the study area (for the 5° interval of 168° - 172°): 3,4%.

By taking this distribution into account, the following sedimentological time scale was obtained: 24 hours (model)  $\equiv$  1 year (prototype). One year in prototype is therefore represented by five cycles, each comprising 3,75 h westerly and 1,05 h easterly waves.

#### 4. CONCLUSIONS

A procedure is outlined for the design of movable bed coastal models, which uses the scales of the longshore and on-offshore transport instead of only longshore transport, as is common practice. This method indicates that sand is preferable to lightweight material for a movable-bed model.

Although the outlined iteration procedure results in large models, the verification is more easily accomplished.

In areas with low sediment transport, it is often possible to acquire good calibration data for a sediment model only if the model includes structures or coastal features that at least partially obstruct the longshore sediment movement. An alternative would be to undertake hydrographic

surveys before and after storms. This, however, can be very costly.

The use of aerial photography for the determination of wave direction provided useful additional coastline data. In this case the photographs were used to identify rocky areas and to obtain waterline growth and recession rates. The main disadvantage of this method is the impossibility of collecting data during stormy periods.

The utilisation of quasi-irregular waves nearly eliminated the formation of beach cusps due to secondary wave effects.

#### 5. ACKNOWLEDGEMENT

The authors gratefully acknowledge the permission given by the consulting engineers, O'Connell, Manthé and Partners, to publish this paper.

#### 6. REFERENCES

- ATKINS, G R (1970). Winds and current patterns in False Bay. Transactions of the Royal Society of South Africa, Vol 39(2), pp 139-148.
- BIJKER, E W (1967). Some considerations about scales for coastal models with movable bed. Delft Hydraulic Laboratory, Publ. No 50, 142 pp.
- CSIR (to be published, 1982a). Valsbaai: velddataverslag (False Bay field data report). Contract Report C/SEA 8219, NRIO, Stellenbosch. (In Afrikaans.)
- CSIR (to be published, 1982b). The effect on the Mvumase project on the Tugela estuary and the adjacent coastline. Contract Report, NRIO, Stellenbosch.
- FAN, L and LE MÉHAUTÉ, B (1969). Final Report. Coastal movable bed scale model technology. Tetra Tech No TC-131, Pasadena, California, 122 pp.
- LONGUET-HIGGINS, M S (1970). Longshore currents generated by obliquely incident sea waves. J of Geophysical Research, Vol 75, No 3.
- SWART, D H (1974). Offshore sediment transport and equilibrium beach profiles. Delft Hydraulic Laboratory, Publ No 131, 302 pp.